Retina

The Dark Atrophy with Indocyanine Green Angiography in Stargardt Disease

Andrea Giani,[1] *Marco Pellegrini,*[1] *Elisa Carini, Antonio Peroglio Deiro, Ferdinando Bottoni, and Giovanni Staurenghi*

Purpose. To evaluate differences in fluorescein angiography (FA) and indocyanine green angiography (ICGA), findings between subjects affected by Stargardt disease (STGD) and atrophic AMD.

Methods. This was a consecutive, cross-sectional case series. A total of 24 eyes of 12 patients with STGD and 23 eyes of 14 patients with atrophic AMD were enrolled in the study. Patients underwent dynamic simultaneous FA and ICGA using a dual beam confocal scanning system. Images were recorded from the initial filling of choroidal and retinal vessels throughout all the phases of the angiogram. Spectral-domain optical coherence tomography (SD-OCT) and fundus autofluorescence were also executed. FA and ICGA findings in the two groups were evaluated.

Results. In 92% (22/24) of eyes affected by STGD, ICGA showed hypocyanescence from the areas of atrophy, more evident in the late phases. This finding, defined as ICGA-imaged "dark atrophy," was present in only 13% (3/23) of the eyes affected by atrophic AMD. The remaining eyes in both groups showed iso- or mild hypercyanescence from the areas of atrophy. Eyes with ICGA-imaged dark atrophy, both in STGD and in atrophic AMD groups, did not show early obscuration of the choroidal vessels by FA. SD-OCT revealed morphologically intact choroid in STGD patients with ICGA-imaged dark atrophy. In atrophic AMD eyes with ICGA-imaged dark atrophy, SD-OCT revealed a severely thinned choroid.

Conclusions. Hypocyanescence by ICGA from the areas of atrophy was more frequent in STGD compared with atrophic AMD. This finding, along with SD-OCT evidence of intact choroid, suggests a possible selective damage of the choriocapillaris in STGD. (*Invest Ophthalmol Vis Sci.* 2012;53:3999–4004) DOI:10.1167/iovs.11-9258

Recessive Stargardt disease (STGD) and age-related macular degeneration (AMD) lead to progressive and severe visual acuity loss. STGD is one of the most common inherited retinal dystrophies, while AMD is the most important cause of central visual acuity loss in western countries. STGD typically appears before age 20. It exhibits simple Mendelian transmission and is caused by mutations in the ABCA4 gene. A reduction in ABCA4 activity in the photoreceptors results in the increased production and accumulation of A2E and related bisretinoids within RPE cells.[1,2] These compounds cannot be readily metabolized and have negative effects on RPE cell function and viability.[2] The result of these pathogenic elements is a progressive loss of RPE and photoreceptors. In contrast, AMD, which typically appears in the sixth decade, has an acquired etiology with a progressive and multifactorial pathology. RPE damage constitutes the initial event.[3,4] RPE cell loss might originate from several mechanisms, including photooxidative stress,[5] vascular alterations,[6,7] and deposition of toxic lipofuscin material under RPE.[1] In the atrophic form of AMD, these alterations lead to progressive loss of RPE and photoreceptor cells.

Fluorescein angiography (FA) and indocyanine green angiography (ICGA) are important tools for diagnostic and pathogenetic evaluation of the two diseases. In STGD, FA is helpful because it allows for the identification of the dark choroid. This finding is characterized by the absence of normal background fluorescence mainly due to the presence of RPE lipofuscin that absorbs the blue excitatory light.[8] Also, ICGA may provide useful information, in particular about the alterations of the choroid and the choriocapillaris.[9] In fact, fluorescein angiography allows accurate imaging of the retinal circulation, but evaluation of the choroidal circulation is limited mainly because of rapid leakage of the dye from fenestrated choriocapillaris that obscures choroidal vessels.[10] In addition, partial absorption by retinal pigment epithelial melanin occurs. In contrast, indocyanine green absorbs and emits light in the near-infrared spectrum, and allows better penetration. Furthermore, indocyanine green is predominantly bound to plasma protein (98% compared with 60%–80% for fluorescein), and this limits its diffusion through the fenestrations of the choriocapillaris.[10]

FA and ICGA studies have suggested vascular abnormalities play a role in the pathogenesis of AMD. In particular, a prolonged choroidal filling phase was associated to atrophic AMD.[11] Moreover, AMD may be characterized by a presumed macular choroidal watershed filling.[12] ICGA showed diminished choroidal arterial perfusion of the macula and enlargement of choroidal veins in the pathogenesis of AMD.[13]

The combination of FA and ICGA facilitates interpretation of the exam and provides more information than either FA or ICGA alone.[10] Therefore, in this study, simultaneous FA and ICGA were used to evaluate possible differences in the pathogenesis of the two clinical entities.

Methods

Twenty-six consecutive patients affected by STGD and atrophic AMD—who were referred to the Department of Clinical Science "Luigi Sacco" from April 2010 to October 2010—were enrolled in the study. Twelve patients were affected by STGD and 14 by atrophic AMD. The study

From the Eye Clinic of Luigi Sacco Hospital, University of Milan, Milan, Italy.

[1]These authors equally contributed to this work and therefore share the first authorship of the paper.

Presented in part at the annual meeting of the Association for Research in Vision and Ophthalmology, Fort Lauderdale, Florida, May 2011.

Submitted for publication December 6, 2011; revised April 10 and May 2, 2012; accepted May 2, 2012.

Disclosure: **A. Giani**, None; **M. Pellegrini**, None; **E. Carini**, None; **A. Peroglio Deiro**, None; **F. Bottoni**, None; **G. Staurenghi**, None

Corresponding author: Giovanni Staurenghi, Eye Clinic, Luigi Sacco Hospital, University of Milan, Via G.B. Grassi, 74 - 20157 Milano; giovanni.staurenghi@unimi.it.

adhered to the tenets of the Declaration of Helsinki and was approved by the local ethics committee. The nature of this study was explained to each of the patients and informed consent was obtained. Each patient underwent a complete ophthalmologic examination, including determination of best-corrected visual acuity (BCVA) using Early Treatment Diabetic Retinopathy Study charts, slit-lamp fundus examination, fundus color photography (Canon CX-1; Canon, Tokyo, Japan), fundus autofluorescence (FAF) by confocal scanning laser ophthalmoscope (cSLO) and spectral-domain optical coherence tomography (SD-OCT) (Spectralis HRA+OCT; Heidelberg Engineering, Heidelberg, Germany). Exclusion criteria included any alternative cause of chorioretinal atrophy in the macular region: pathologic myopia; pattern dystrophies; central areolar macular atrophy; rod-cone dystrophy; retinitis pigmentosa; drug-induced retinopathy; Best disease, adult-onset vitelliform dystrophy; Sorsby macular dystrophy; solar retinopathy; chorioretinal inflammatory diseases; and post-traumatic atrophy. In addition, patients were excluded if they had previous retinal laser treatments and retinal surgery, choroidal neovascularization, and any retinal vascular pathology.

Diagnostic criteria for STGD included decreased visual acuity before age 35 associated with multiple fundus flecks, atrophic lesions within the macula, and diagnosis confirmation by ABCA4 genotyping. Diagnostic criteria for atrophic AMD were age $\geq$50 years and evidence of unifocal or multifocal areas of RPE loss in at least one eye. If both eyes met the inclusion criteria, both eyes were included. Patients with late-onset disease ($\geq$50 years) who showed the "diffuse-fine granular with peripheral punctate spots" phenotype were excluded because this condition may represent a late onset STGD mimicking atrophic AMD.[14] Each patient underwent dynamic, simultaneous FA and ICGA using a cSLO (Heidelberg Engineering). One milliliter of a solution containing 25 mg of indocyanine green (Pulsion, Munich, Germany) mixed with 5 mL of 20% fluorescein (500 mg, Monico SPA, Venezia, Italy) was injected followed by a 5-mL saline solution flush. Recording of the images with the movie modality (8 images/s) was started immediately after the injection of the mixed dyes. Notably, the software automatically recorded from 2 seconds before the start of the movie. If both eyes were included in the study, the eye with the worst visual acuity was chosen for movie acquisition. Recording continued until the filling of the choriocapillaris and choroidal and retinal vessels was completed. After that, FA and ICGA images were acquired in both eyes until late phase, at least 40 minutes after injection.

FA and ICGA images from the initial filling of the vessels throughout all phases of the exam were analyzed. In particular, the intensity of the fluorescence from the atrophic lesions was compared with the background and classified as hypo-, iso-, or hyperfluorescent for FA, and hypo-, iso-, or hypercyanescent for ICGA. SD-OCT images were analyzed to evaluate retinal morphology and choroidal alterations beneath the area of atrophy.

The areas of atrophy were manually measured in FAF images using the dedicated confocal scanning software (Heidelberg Engineering). Two independent examiners performed the measurements, and values were compared with paired *t*-tests to assess interoperator variability. Areas of atrophy by FAF were then classified as "small" or "large," based upon the median value. Afterwards, the presence of hypocyanescent atrophy was correlated with the extent of atrophy by FAF and the type of disease. This analysis was performed using a log-linear model: Evidence of hypocyanescent atrophy was considered the independent variable, while the extension of atrophy by FAF and the type of disease were set as dependent variables. For statistical analysis, study authors used R language statistics software (http://www.r-project.org, in the public domain; last accessed March 27, 2012).

Results

Both eyes of all 12 STGD patients (4 males and 8 females) were included in the study. The mean age was 50 years (range 17–78 years), and the mean BCVA was 20/100 (range 20/500–20/25). In all of the patients, the STGD diagnosis was confirmed by identification of at least one mutation in ABCA4. Sixteen of the 24 eyes (77%) presented geographic atrophy at the posterior pole. The remaining 8 eyes had a pattern of multiple, discrete, nonconfluent areas of atrophy.

Twenty-three eyes of the 14 atrophic AMD patients (6 males and 8 females) were included in the study. The mean age was 75 years (range 60–86 years), and the mean BCVA was 20/63 (range 20/500–20/20). Sixteen of the 23 eyes (70%) presented geographic atrophy at the posterior pole. The remaining 7 eyes showed a pattern of multiple, discrete areas of atrophy.

ICGA showed hypocyanescence from the areas of atrophy in 92% (22/24) of eyes affected by STGD and in 13% (3/23) of eyes affected by atrophic AMD. This hypocyanescence in the affected portions of the macula was defined as ICGA-imaged "dark atrophy" (Figs. 1A–D). All the remaining eyes showed isocyanescence or mild hypercyanescence from the areas of atrophy in the late phase of ICGA (Figs. 1E–1H). Within the 22 eyes affected by STGD with ICGA-imaged dark atrophy, 16 (73%) showed no dye leakage from the choriocapillaris during dynamic FA (Fig. 2, *top row*). The 6 remaining eyes showed leakage from the choriocapillaris on FA. All the eyes affected by atrophic AMD with no evidence of ICGA-imaged dark atrophy showed prompt dye leakage from the choriocapillaris during dynamic FA (Fig. 2, *bottom row*). In the 3 eyes affected by atrophic AMD with ICGA-imaged dark atrophy, dynamic FA showed no dye leakage from the choriocapillaris.

Evidence of a dark choroid, defined as a wide-field absence of the normal background in FA images, was present in 75% (18/24) of the patients affected by STGD. In the remaining 6 STGD patients with no evidence of dark choroid by FA, ICGA-imaged dark atrophy was always present as revealed by ICGA. No patient with atrophic AMD showed evidence of dark choroid.

SD-OCT images showed a morphologically intact choroid in 91% (20/22) of the eyes affected by STGD with ICGA-imaged dark atrophy (Fig. 3A). Eyes affected by atrophic AMD with no evidence of ICGA-imaged dark atrophy showed the same finding, with intact choroidal thickness (Fig. 3B). Also, in the two eyes affected by STGD with no evidence of ICGA-imaged dark atrophy, SD-OCT showed the same finding, with normal choroidal thickness (Fig. 4). On the contrary, in eyes affected by atrophic AMD with evidence of ICGA-imaged dark atrophy, SD-OCT showed evident choroidal thinning underneath the areas of atrophy (Fig. 5).

The mean area of atrophy by FAF was 15.96 ± 20.98 mm^2 in patients affected by STGD and 10.12 ± 5.08 mm^2 in patients affected by atrophic AMD (Student's *t*-test, $P = 0.19$). No difference was found between measurements executed by the two different operators ($P = 0.68$). The presence of ICGA-imaged dark atrophy was strongly correlated with the diagnosis of STGD ($P < 0.001$). No correlation between the presence of ICGA-imaged dark atrophy and extent of atrophy by FAF was found for both STGD and AMD patients ($P = 0.19$).

Discussion

In this study, the frequency of dark atrophy, defined as hypocyanescence by ICGA within the area of macular atrophy, was remarkably high, 92%, in patients with STGD. The finding of hypocyanescence by ICGA in STGD is in accordance with observations by Schwoerer et al.[9] Using ICGA, they found a characteristic pattern of small, clearly demarcated, hypocyanescent areas in STGD patients. The results are even more interesting when compared with the low frequency observed in patients with atrophic AMD: 13%. Moreover, within the patients affected by STGD with no evidence of dark choroid,

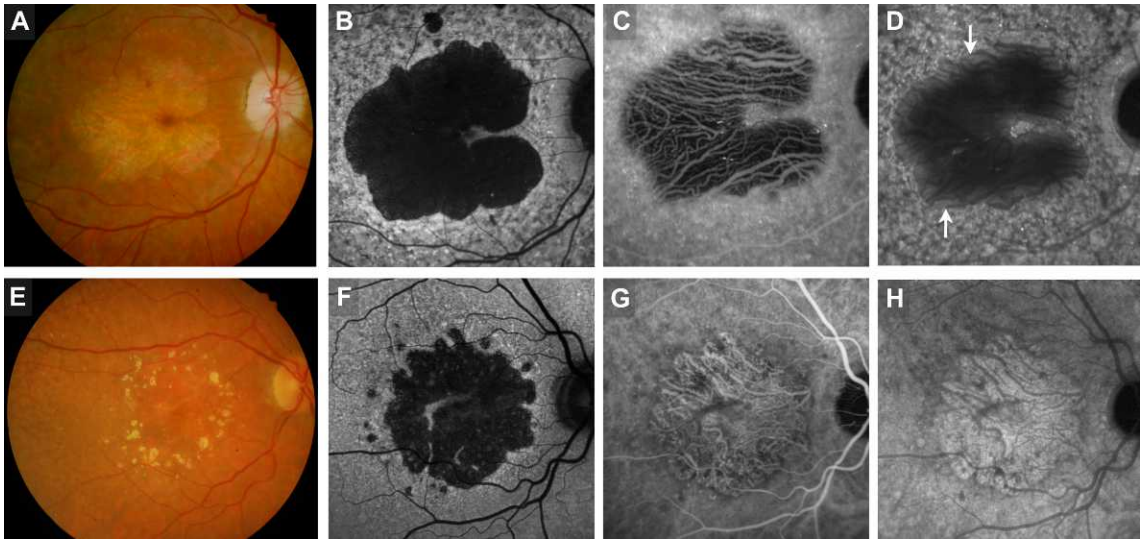

Figure 1. Comparison between a patient affected by STGD (**A**–**D**) and a patient affected by atrophic AMD (**E**–**H**). Patient with STGD was a 54-year-old woman that began to have vision loss in both eyes at age 22. Her visual acuity was 20/40 in the right eye and 20/32 in the left eye. Genetic analysis revealed the presence of the mutations in the ABCA4 gene: c.635G > A (p.Arg212His) (het); c.4594G > A (pAsp1532Asn) (het); c.6088C > T (p.Arg2030term) (het). Patient with atrophic AMD was referred to clinic in 2005. At the first presentation, he had multiple areas of RPE and photoreceptor damage in the posterior pole of both eyes, sparing the fovea. During the follow-up, the areas of RPE and photoreceptor alteration enlarged, becoming atrophic and confluent. At the study visit, he presented geographic atrophy in both eyes, partially involving the fovea. His visual acuity was 20/32 in the right eye and 20/25 in the left eye. In both cases, fundus color photographs show geographic atrophy and diffuse yellowish deposits in the posterior pole (**A**, **E**), which corresponded to flecks in STGD and to drusen in atrophic AMD. These lesions were much more visible with autofluorescence images (**B**, **F**), in which the area of atrophy was readily visible due to the absence of the RPE. Intermediate (6 minutes; **C**, **G**) and late (40 minutes; **D**, **H**) phases of ICGA show very different aspects of the atrophy. In STGD, this area is hypocyanescent (**C**, **D**); while in atrophic AMD, the area of atrophy was isocyanescent in the intermediate phase and became slightly hypercyanescent in the late phase (**G**, **H**). In STGD, late-phase ICGA showed more cyanescence from the border of the atrophy compared with the central part of the atrophy (**D**, *white arrows*).

ICGA-imaged dark atrophy was always present. This indicates a possible role for differential diagnosis and, more importantly, suggests additional differences in the pathogenesis of the two diseases.

One explanation for the ICGA-imaged dark atrophy may be the presence of material that obscures ICGA cyanescence. However, this hypothesis seems unlikely, since SD-OCT images failed to show any deposit between the choroid and the retina. Moreover, the window defects visible in SD-OCT images under the areas of atrophy (Fig. 3A, *white arrows*) suggest that the near-infrared light is able to visualize deeper choroidal layers. Since in the confocal scanning software (Heidelberg Engineering) the wavelength used to get SD-OCT images is similar to the spectrum of cyanescence from ICGA, the presence of these window defects might exclude any blockage of ICGA-cyanescent light.

Another hypothesis on the origin of the ICGA-imaged dark atrophy is an extended damage of choriocapillaris. The findings

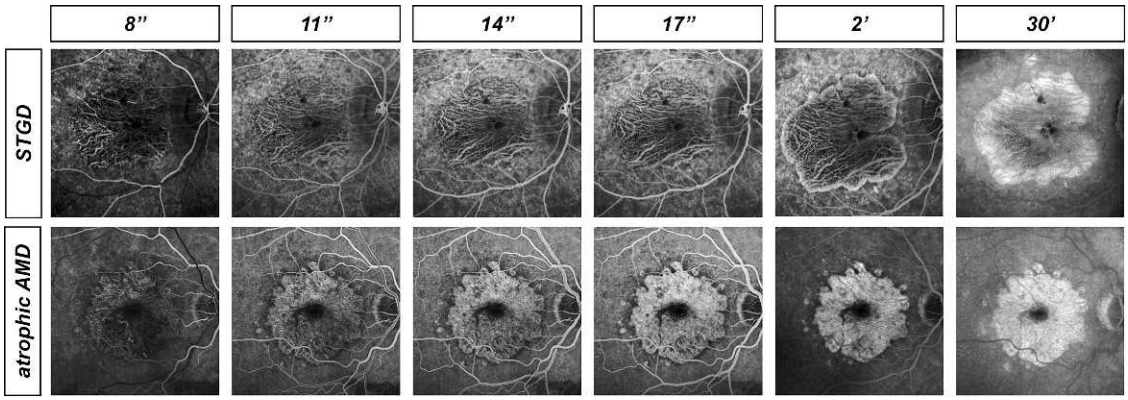

Figure 2. Comparison of dynamic fluorescein angiography images between the same patients showed in Figure 1. The first patient (*top row*) was affected by STGD, while the second patient (*bottom row*) was affected by atrophic AMD. The images at 8, 11, 14, and 17 seconds after the injection, as well as at 2 and 30 minutes are shown. In the very early phases of the angiograms (8 seconds), in both cases the medium-to-large choroidal vessels were visible because the dye had not reached the choriocapillaris layer yet. In the following phases though, the angiograms started to show a different evolution. In STGD, there was no obscuration of choroidal vessels at 11, 14, 17 seconds, and 2 minutes. In contrast, for atrophic AMD, the diffusion of the fluorescein throughout the choriocapillaris lead to early obscuration of medium-to-large choroidal vessels, which were barely visible from 11 to 17 seconds, and at 2 and 30 minutes. The intermediate (2 minutes) and late (30 minutes) phases of the angiogram show a different aspect of the two pathologies. In STGD, the borders of the area of atrophy became progressively hyperfluorescent, while the center was iso-hypofluorescent. In atrophic AMD, the entire area of atrophy was uniformly hyperfluorescent.

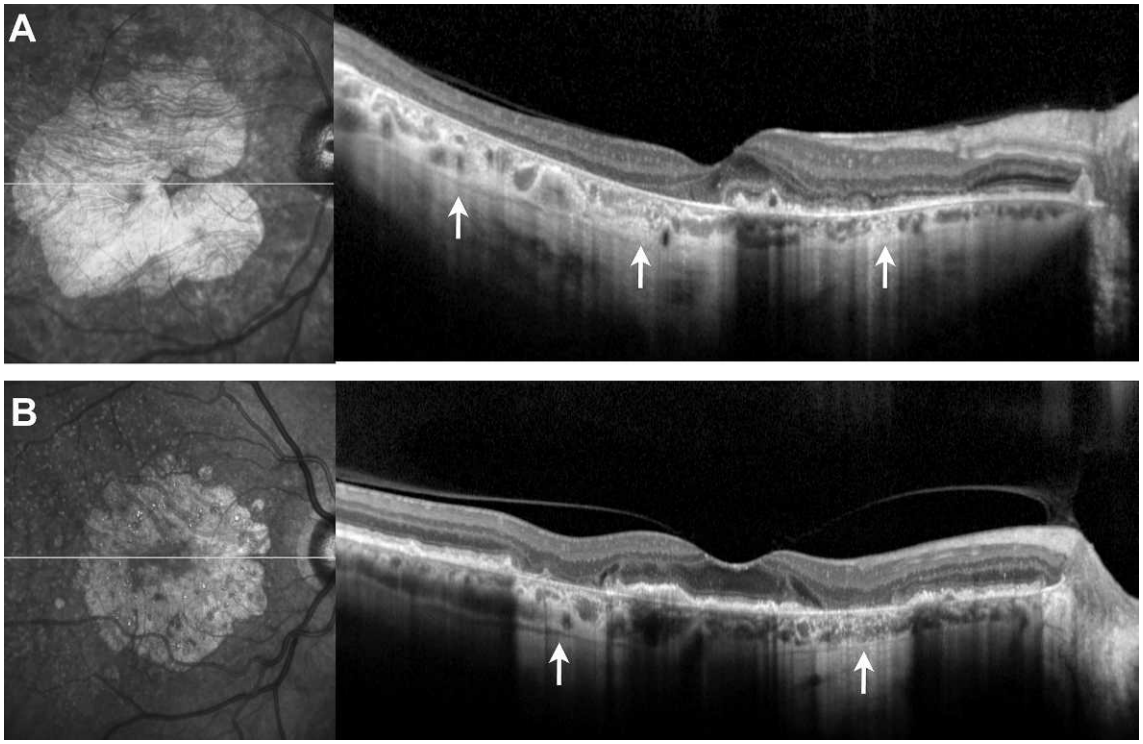

Figure 3. Comparison of SD-OCT findings in the same patients shown in Figure 1. The first patient (**A**) was affected by STGD, while the second patient (**B**) was affected by atrophic age-related macular degeneration. The SD-OCT sections passed through the lines displayed in the corresponding scanning laser ophthalmoscopic infrared images on the left. The choroid beneath the atrophy (*white arrows*) did not show major alterations, and no evident differences between the two cases were visible.

in FA images seem to corroborate this hypothesis because the absence of dye leakage from the early phases of the angiogram may be explained by the absence of capillaries. In FA images, the border of atrophy in STGD often showed some degree of hyperfluorescence. Also ICGA late phases revealed an increase in cyanescence from the border of the atrophy. The fact that these findings start to appear in the intermediate phases and are much more evident in the late phases may indicate that they originate from choriocapillaris surrounding the area of atrophy, rather than beneath it. The choroid and choriocapil-

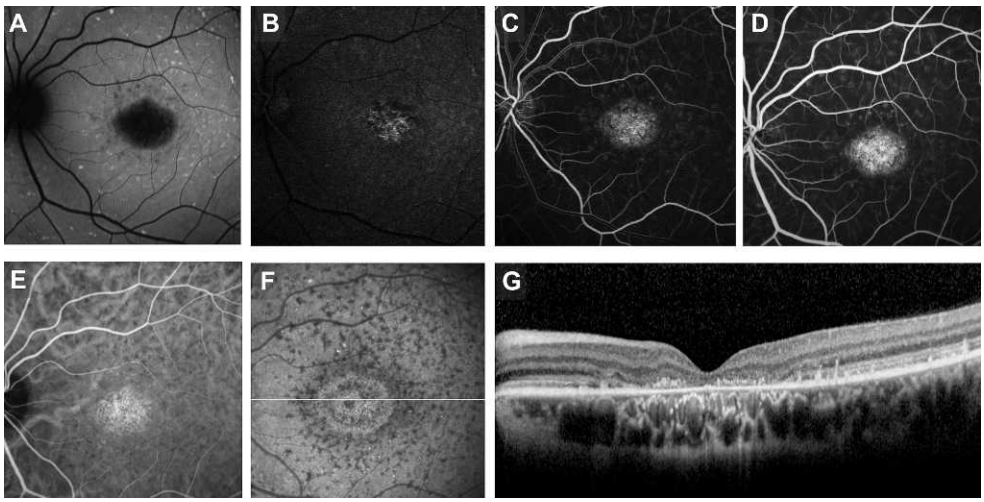

Figure 4. A case of STGD without ICGA-imaged dark atrophy. The patient was a 17-year-old woman that began suffering with metamorphopsia and visual loss at the age of 8. At the study visit, she presented photoreceptor and RPE atrophy, with a visual acuity of 20/125 in both eyes. The diagnosis of STGD was confirmed after genetic analysis of the ABCA4 gene, which revealed the following mutations: c.2099G > A (p.Trp700Term) (het); c.2588G > C (p.Gly863Ala) (het). Autofluorescence imaging (**A**) showed a central area of atrophy and hyperautofluorescent flecks at the posterior pole and midperiphery. Very early-phase FA (**B**) showed filling of the choroidal vessels, evident in the corresponding area of central atrophy. In the venous phase of the angiogram (**C**) and in the following phases of the exam (**D**), leakage of fluorescein out of the choriocapillaris obscured the visualization of choroidal vessels. ICGA showed hypercyanescence from the area of atrophy in early and intermediate phases (**E**), and isocyanescence in the late phase (**F**). The SD-OCT section (**G**) passing through the line in Figure 4F showed no major alteration of the choroid and some deposition of material in the outer retinal layers.

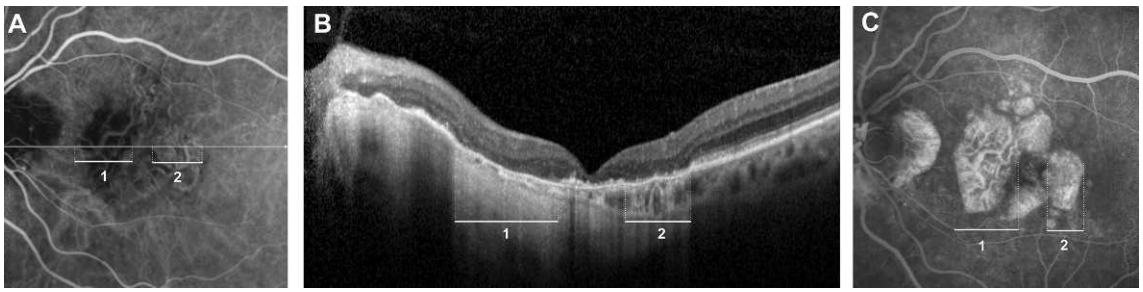

Figure 5. A case of atrophic AMD with ICGA-imaged dark atrophy. The patient was an 86-year-old woman. She was first seen in the clinic in 2008 for drusen with RPE defects in both eyes and an extrafoveal area of RPE atrophy in her left eye. During the following years, the patient developed an extrafoveal area of atrophy in the right eye. In her left eye, the atrophy enlarged and merged with other new areas of RPE and photoreceptor loss. At the time of the visit, the geographic atrophy in her left eye partially involved the foveal region, which presented a thinning of the neuroretina. The visual acuity was 20/32 in the right eye and 20/500 in the left eye. ICGA (**A**) showed different aspects of two areas of atrophy. The area nasal to the fovea was hypocyanescent (**A**, *line 1*); while temporal to the fovea (**A**, *line 2*), the atrophy was iso-hypercyanescent. The SD-OCT image showed a different aspect of the choroid beneath the two zones of atrophy. Corresponding with the first area (**B**, *line 1*) the choroid was extremely thinned; while beneath the second area (**B**, *line 2*), the choroid was still present and morphologically intact. FA was also different. In the nasal area of atrophy (**C**, *line 1*), the image visualized the medium-to-large choroidal vessels, while in the temporal area (**C**, *line 2*) the choroidal vessels were obscured by diffusion of the dye.

laris atrophy in the late stages of the disease.[15–17] Moreover, the absence of normal choroidal hyperfluorescence by FA in the final stages of STGD was previously described by Lopez et al.[18] The authors stated that this "choroidal silence" has to be differentiated from the dark choroid. In fact, the first is due to marked atrophy of the choriocapillaris, while the second originates with the angiographic blockage by lipofuscin in RPE.[18]

Choriocapillaris atrophy is a direct consequence of RPE absence. In fact, these two structures share a mutualistic relationship. When one component is affected, either or both may degenerate.[19,20] RPE produces VEGF that stimulates the angiogenesis and the formation of fenestrations.[21] Moreover, VEGF is secreted from the basal part of the RPE cells, and VEGF receptors are expressed in the choroidal endothelium facing the RPE.[22] Several studies have underlined the pathogenic relevance of choroidal vascular alterations in AMD.[4,5,23–25] Vascular density has been reported to either decrease[26] or modestly increase.[27,28] However, McLeod et al. did not observe complete loss of choriocapillaris beneath areas of total RPE atrophy in atrophic AMD eyes, even though the RPE atrophy had been documented clinically for 20 years.[4,20] This is consistent with what was observed in this study, in patients affected by atrophic AMD. In the majority of the cases, FA images showed an early diffusion of the dye in the area of atrophy, suggesting the presence of some residual capillaries. In contrast, there was an absence of fluorescein leakage in STGD patients with ICGA-imaged dark atrophy, suggesting a complete loss of the choriocapillaris. A previous study evaluated the extension of the areas of atrophy in patients affected by STGD using 488-nm and 787-nm FAF.[29] The authors found that 787-nm FAF always showed a more widespread area of atrophy, compared with 488-nm FAF. Since 787-nm FAF is primarily produced by melanin, the most likely explanation of this finding is that in STGD, the melanin distribution within RPE cells may be altered before cellular loss occurs.[29] However, in addition to a contribution from the RPE, 787-nm FAF also originates from the choroid.[30] For this reason, another possible explanation of the more widespread areas of atrophy visible with 787-nm FAF may be a selective damage of the choriocapillaris in STGD, which is in accordance with this study's findings.

The different conditions of the choriocapillaris may be due to different stages of the two diseases, especially in terms of RPE and choriocapillaris loss. By definition, STGD has an earlier age of onset. Therefore, in these patients, there may be more time for the RPE to degenerate, with consequently more extended choriocapillaris atrophy. Moreover, considering the different pathogenesis of the two diseases, it cannot be excluded that in STGD, RPE and choriocapillaris death occurs more rapidly. This may lead to the more frequent finding of ICGA-imaged dark atrophy in these patients. However, no correlation between the evidence of ICGA-imaged dark atrophy and the extension of RPE atrophy by FAF was found in this study. This result, in addition to the strong correlation between ICGA-imaged dark atrophy and STGD from the same analysis, suggests that with a similar grade of atrophy, the presence of ICGA-imaged dark atrophy is influenced only by the diagnosis.

When ICGA-imaged atrophy was present in patients with atrophic AMD, SD-OCT images displayed a nearly complete atrophy of the whole choroidal layer. In contrast to that, the choroid under the areas of atrophy in STGD patients seemed to be morphologically intact. This sparing of the choroid was also shown by histopathological studies of fundus flavimaculatus, which is considered to be a milder form of STGD.[5,18,31–34] In contrast, a loss of choriocapillaris with intact choroid was observed in aggressive and early-onset cases,[31,32] which is in accordance with study findings. It is important to note that an intact choroid on SD-OCT does not necessarily indicate an intact choriocapillaris. In fact, SD-OCT technology is not yet sensitive enough for clear distinguishing choriocapillaris from choroid. Conversely, while it is logical to assume that choroidal atrophy on SD-OCT implies loss of choriocapillaris, the imaging alone does not prove this.

In conclusion, hypocyanescence with ICGA from the areas of atrophy is much more frequent in STGD compared with atrophic AMD. This finding, together with evidence of a relatively intact choroid and with the lack of leakage shown by FA, seems to suggest a possible direct damage to the choriocapillaris in STGD.

Acknowledgments

The authors thank Mario Cigada for professional statistical assistance, and Magi Onlus for genetic analysis and DNA sequencing.

References

1. Sparrow JR, Kim SR, Cuervo AM, Bandhyopadhyayand U. A2E, a pigment of RPE lipofuscin, is generated from the precursor,

A2PE by a lysosomal enzyme activity. *Adv Exp Med Biol*. 2008; 613:393–398.

2. Weng J, Mata NL, Azarian SM, Tzekov RT, Birch DG, Travis GH. Insights into the function of Rim protein in photoreceptors and etiology of Stargardt's disease from the phenotype in abcr knockout mice. *Cell*. 1999;98:13–23.
3. Bearelly S, Chau FY, Koreishi A, Stinnett SS, Izatt JA, Toth CA. Spectral domain optical coherence tomography imaging of geographic atrophy margins. *Ophthalmology*. 2009;116:1762–1769.
4. McLeod DS, Taomoto M, Otsuji T, Green WR, Sunness JS, Lutty GA. Quantifying changes in RPE and choroidal vasculature in eyes with age-related macular degeneration. *Invest Ophthalmol Vis Sci*. 2002;43:1986–1993.
5. Beatty S, Koh H, Phil M, Henson D, Boulton M. The role of oxidative stress in the pathogenesis of age-related macular degeneration. *Surv Ophthalmol*. 2000;45:115–134.
6. Hageman GS, Anderson DH, Johnson LV, et al. A common haplotype in the complement regulatory gene factor H (HF1/CFH) predisposes individuals to age-related macular degeneration. *Proc Natl Acad Sci U S A*. 2005;102:7227–7232.
7. Lutty G, Grunwald J, Majji AB, Uyama M, Yoneya S. Changes in choriocapillaris and retinal pigment epithelium in age-related macular degeneration. *Mol Vis*. 1999;5:35.
8. Fish G, Grey R, Sehmi KS, Bird AC. The dark choroid in posterior retinal dystrophies. *Br J Ophthalmol*. 1981;65:359–363.
9. Schwoerer J, Secretan M, Zografos L, Piguet B. Indocyanine green angiography in Fundus flavimaculatus. *Ophthalmologica*. 2000;214:240–245.
10. Holz FG, Bellmann C, Rohrschneider K, Burk RO, Volcker HE. Simultaneous confocal scanning laser fluorescein and indocyanine green angiography. *Am J Ophthalmol*. 1998;125:227–236.
11. Pauleikhoff D, Spital G, Radermacher M, Brumm GA, Lommatzsch A, Bird AC. A fluorescein and indocyanine green angiographic study of choriocapillaris in age-related macular disease. *Arch Ophthalmol*. 1999;117:1353–1358.
12. Ross RD, Barofsky JM, Cohen G, Baber WB, Palao SW, Gitter KA. Presumed macular choroidal watershed vascular filling, choroidal neovascularization, and systemic vascular disease in patients with age-related macular degeneration. *Am J Ophthalmol*. 1998;125:71–80.
13. Mori K, Gehlbach PL, Ito YN, Yoneya S. Decreased arterial dye-filling and venous dilation in the macular choroid associated with age-related macular degeneration. *Retina*. 2005;25:430–437.
14. Scholl HP, Fleckenstein M. Charbel Issa P, Keilhauer C, Holz FG, Weber BH. An update on the genetics of age-related macular degeneration. *Mol Vis*. 2007;13:196–205.
15. Klevering BJ, Deutman AF, Maugeri A, Cremers FP, Hoyng CB. The spectrum of retinal phenotypes caused by mutations in the ABCA4 gene. *Graefes Arch Clin Exp Ophthalmol*. 2005; 243:90–100.
16. Armstrong JD, Meyer D, Xu S, Elfervig JL. Long-term follow-up of Stargardt's disease and fundus flavimaculatus. *Ophthalmology*. 1998;105:448–457.
17. Rotenstreich Y, Fishman GA, Anderson RJ. Visual acuity loss and clinical observations in a large series of patients with Stargardt disease. *Ophthalmology*. 2003;110:1151–1158.
18. Lopez PF, Maumenee IH, de la Cruz Z, Green WR. Autosomal-dominant fundus flavimaculatus. Clinicopathologic correlation. *Ophthalmology*. 1990;97:798–809.
19. Henkind P, Gartner S. The relationship between retinal pigment epithelium and the choriocapillaris. *Trans Ophthalmol Soc U K*. 1983;103:444–447.
20. McLeod DS, Grebe R, Bhutto I, Merges C, Baba T, Lutty GA. Relationship between RPE and choriocapillaris in age-related macular degeneration. *Invest Ophthalmol Vis Sci*. 2009;50: 4982–4991.
21. Adamis AP, Shima DT, Yeo KT, et al. Synthesis and secretion of vascular permeability factor/vascular endothelial growth factor by human retinal pigment epithelial cells. *Biochem Biophys Res Commun*. 1993;193:631–638.
22. Blaauwgeers HG, Holtkamp GM, Rutten H, et al. Polarized vascular endothelial growth factor secretion by human retinal pigment epithelium and localization of vascular endothelial growth factor receptors on the inner choriocapillaris. Evidence for a trophic paracrine relation. *Am J Pathol*. 1999;155: 421–428.
23. Grunwald JE, Hariprasad SM, DuPont J, et al. Foveolar choroidal blood flow in age-related macular degeneration. *Invest Ophthalmol Vis Sci*. 1998;39:385–390.
24. Mullins RF, Johnson MN, Faidley EA, Skeie JM, Huang J. Choriocapillaris vascular dropout related to density of drusen in human eyes with early age-related macular degeneration. *Invest Ophthalmol Vis Sci*. 2011;52:1606–1612.
25. Yoneya S, Saito T, Komatsu Y, Koyama I, Takahashi K, Duvoll-Young J. Binding properties of indocyanine green in human blood. *Invest Ophthalmol Vis Sci*. 1998;39:1286–1290.
26. Ramrattan RS, van der Schaft TL, Mooy CM, de Bruijn WC, Mulder PG, de Jong PT. Morphometric analysis of Bruch's membrane, the choriocapillaris, and the choroid in aging. *Invest Ophthalmol Vis Sci*. 1994;35:2857–2864.
27. Spraul CW, Lang GE, Grossniklaus HE. Morphometric analysis of the choroid, Bruch's membrane, and retinal pigment epithelium in eyes with age-related macular degeneration. *Invest Ophthalmol Vis Sci*. 1996;37:2724–2735.
28. Spraul CW, Lang GE, Grossniklaus HE, Lang GK. Histologic and morphometric analysis of the choroid, Bruch's membrane, and retinal pigment epithelium in postmortem eyes with age-related macular degeneration and histologic examination of surgically excised choroidal neovascular membranes. *Surv Ophthalmol*. 1999;44(suppl):S10–S32.
29. Kellner S, Kellner U, Weber BH, Fiebig B, Weinitz S, Ruether K. Lipofuscin- and melanin-related fundus autofluorescence in patients with ABCA4-associated retinal dystrophies. *Am J Ophthalm*ol. 2009;147:895–902.
30. Keilhauer CN, Delori FC. Near-infrared autofluorescence imaging of the fundus: visualization of ocular melanin. *Invest Ophthalmol Vis Sci*. 2006;47:3556–3564.
31. Birnbach CD, Jarvelainen M, Possin DE, Milam AH. Histopathology and immunocytochemistry of the neurosensory retina in fundus flavimaculatus. *Ophthalmology*. 1994;101:1211–1219.
32. Eagle RCJ, Lucier AC, Bernardino VBJ, Yanoff M. Retinal pigment epithelial abnormalities in fundus flavimaculatus: a light and electron microscopic study. *Ophthalmology*. 1980; 87:1189–1200.
33. McDonnell PJ, Kivlin JD, Maumenee IH, Green WR. Fundus flavimaculatus without maculopathy. A clinicopathologic study. *Ophthalmology*. 1986;93:116–119.
34. Steinmetz RL, Garner A, Maguire JI, Bird AC. Histopathology of incipient fundus flavimaculatus. *Ophthalmology*. 1991;98: 953–956.